Type II/III cell composition and NCAM expression in taste buds

Eriko Koyanagi-Matsumura†, Hirohito Miura†, Mitsuru Saito, Shuitsu Harada

Oral Physiology, Kagoshima University Graduate School of Medical and Dental Sciences, 8-35-1 Sakuragaoka, Kagoshima-shi, Kagoshima 890-8544, Japan.

† These authors equally contributed to this work.

Corresponding to be sent to:

Hirohito Miura,

E-mail: hmiura@dent.kagoshima-u.ac.jp,

Tel: +81-99-275-6122 (ext 6121)

Fax: +81-99-275-6128

Acknowledgements:

The authors thank Dr. Ayumi Nakayama for technical support for whole mount immunohistochemistry and Dr. John Caprio for valuable comments on the manuscript.

Funding:

This work was supported by Japan Society for the Promotion of Science (JSPS) KAKENHI Grant Numbers JP17K11647 and JP20K09892 to HM.

Abstract

Taste buds are localized in fungiform (FF), foliate (FL), and circumvallate (CV) papillae on the tongue and taste buds also occur on the soft palate (SP). Mature elongate cells within taste buds are constantly renewed from stem cells and classified into three cell types, Type I, II, and III. These cell types are generally assumed to reside in respective taste buds in a particular ratio corresponding to taste regions. A variety of cell-type markers were used to analyze taste bud cells. NCAM is the first established marker for Type III cells and is still often used. However, NCAM was examined mainly in the CV, but not sufficiently in other regions. Furthermore, our previous data suggested that NCAM may be transiently expressed in the immature stage of Type II cells. To precisely assess NCAM expression as a Type III cell marker, we first examined Type II and III cell-type markers, IP3R3 and CA4, respectively, and then compared NCAM with them using whole-mount immunohistochemistry. IP3R3 and CA4 were segregated from each other, supporting the reliability of these markers. The ratio between Type II and III cells varied widely among taste buds in the respective regions (Pearson's r =0.442 [CV], 0.279 [SP], and -0.011[FF]), indicating that Type II and III cells are contained rather independently in respective taste buds. NCAM immunohistochemistry showed that a subset of taste bud cells were NCAM(+)CA4(-). While NCAM(+)CA4(-) cells were IP3R3(-) in the CV, the majority of them were IP3R3(+) in the SP and FF.

Key words: cell type marker, taste cell differentiation, whole-mount immunohistochemistry, regional difference, stem/progenitor cell

Introduction

Gustation, or the sense of taste, tells animals what to expect from eating potential food items and regulates ingestion. Each taste quality represents distinct signs. In general, sweet, umami, and moderately salty indicate beneficial nutrients providing energy and homeostatic balance. Bitter and

sour mean potentially harmful items, poisonous or spoiled ones. Taste buds, the sensory end organ for gustation, are composed of 50-100 cells and are localized in three taste papillae of the tongue [fungiform (FF), foliate (FL), and circumvallate (CV)] and on the soft palate (SP) in the oral cavity. Taste bud cells are constantly renewed from local epithelial stem cells (Beidler and Smallman 1965; Farbman 1980; Stone et al. 1995; Barlow and Northcutt 1995), which are bipotential and produce taste bud cells and also epithelial cells that surround taste buds (Okubo et al. 2009; Miura et al. 2014). The homeostasis of taste buds during cell turnover is essential for the consistency of gustatory function. Within taste buds, elongate cells are mature cells and are classified into three cell types, Type I, II, and III, originally based on morphological features observed by electron microscopy (Finger and Simon 2000). It is generally assumed that in taste buds Type I cells are most abundant, followed by Type II cells and the least frequent Type III cells (Chaudhari and Roper 2010; Barlow and Klein 2015).

Currently, it is established that each cell type contains taste cells dedicated to the response to specific taste qualities: Type II to sweet, umami, and bitter; Type III to sour (Kinnamon and Finger 2019). Subsets of Type II and Type III cells are also involved in the detection of aversive high-concentrations of salty stimuli (Oka et al. 2013). Type I cells are generally considered as glial-like cells expressing ecto-ATPase on the cell membrane, which hydrolyzes ATP secreted as an afferent taste neurotransmitter (Finger et al. 2005; Bartel et al. 2006; Taruno et al. 2013; Ma et al. 2018). Type I cells have been also referred to as cells responding to low-concentrations of salty stimuli since no molecular or functional indication for Type II or III cells was found in taste cells responding to low-salt (Bachmanov et al. 2002; Chandrashekar et al. 2010; Shigemura and Ninomiya 2016). Recently, GAD65-expressing Type I cells were shown to actually respond to low-salt (Baumer-Harrison et al. 2020). Besides taste cells responsive to specific taste qualities, a subset of Type III cells are shown to respond to multiple taste qualities (Tomchik et al. 2007). Although the sensitivity of Type III cells to multiple qualities was assumed to be mediated via input from Type II cells (Roper and Chaudhari 2017), it was recently shown that about half of Type III

cells directly respond to bitter, sweet, and/or umami in addition to sour (Banik et al. 2020). Knowledge of the heterogeneities of taste bud cells is steadily growing, increasing the importance of the precise characterization of the specificity and coverage of cell type-specific markers. The overlapping and segregated patterns of various molecules expressed within taste buds are also thought to provide important clues for taste cell differentiation and lineage relationships among taste bud cells.

Several molecules have been used as markers to analyze Type III cells, including NCAM (Takeda et al. 1992; Nelson and Finger 1993; Yee et al. 2001), serotonin (5-HT) (Kim and Roper 1995), synaptosomal-associated protein 25 (SNAP25) (Yang et al. 2000; Clapp et al. 2006), glutamic acid decarboxylase 67 (GAD67) (DeFazio et al. 2006; Tomchik et al. 2007; Dvoryanchikov et al. 2011), polycystic kidney disease 2-like 1 protein (PKD2L1) (Huang et al. 2006; Ishimaru et al. 2006; Kataoka et al. 2008), aromatic L-amino-acid decarboxylase (AADC), chromogranin A (ChrgA) (Dvoryanchikov et al. 2007), and carbonic anhydrase isoform 4 (CA4) (Chandrashekar et al. 2009). The single cell RNAseq study showed that many of these markers enriched in individual Type III cells (Sukumaran et al. 2017). Recently, regional differences were reported in the colocalization of these molecules (Lossow et al. 2017; Wilson et al. 2017). Wilson *et al.* compared PKD2L1 versus 5-HT, SNAP25, and GAD67 and revealed that Type III cells are more diverse in the expression pattern of these molecules in the FF and SP than those in the CV and FL. Lossow et al. compared CA4 versus AADC, SNAP25, and GAD67 and demonstrated that CA4 almost completely overlapped with these molecules in the FF and SP; further CA4(+) cells were contained in 80-90% of the taste cells expressing the other markers in the CV and FL, implying that CA4(+) cells may represent the core population, which express all markers for Type III cells. Although these observations are expanding our understanding of the regional differences in the heterogeneity of Type III cells, there remain other molecular markers that require examination more extensively, including NCAM, the first established marker for Type III cells. The expression of NCAM was examined mainly in the CV, but not sufficiently in other regions. Furthermore, our

previous data obtained by the combination of immunohistochemistry for NCAM and *in situ* hybridization for Type II markers suggested the possibility that NCAM is transiently expressed in very early stages of the differentiation of Type II cells (Miura et al. 2005, 2006).

In the present study, we examined the expression of NCAM in the CV, FF, and SP using whole-mount immunohistochemistry of peeled epithelium. To assess cell-type specificity, IP3R3 and CA4 were used as Type II and III cell markers, respectively. We first confirmed the segregated expression of these cell-type markers and showed a vast diversity in the ratio between Type II and III cells among taste buds in respective taste regions. We showed NCAM(+)CA4(-) cells in taste buds. NCAM(+)CA4(-) cells were IP3R3(-) in the CV while the majority were IP3R3(+) in the SP and FF. We also assessed the impact of the occurrence of NCAM(+)CA4(-) cells to other cells within taste buds.

Materials and Methods

Experimental animals and Tissue preparation for whole-mount immunohistochemistry

The animals used in this experiment were male C57BL/6J mice (9-20 weeks of age) purchased from Japan SLC, Inc. (Hamamatsu, Japan). Animals were sacrificed by injection of an excessive dose of sodium pentobarbital (250 mg/kg, intraperitoneally; Nacalai Tesque, Inc., Kyoto, Japan). All experimental procedures were approved by the institutional animal care and use committees and were conducted at Kagoshima University.

Whole-mount immunohistochemistry was performed as previously described with some modifications (Miura et al. 2007). The tongue was excised and put into phosphate buffered saline (PBS; pH7.4), and the soft palate was rinsed with PBS. Ringer's solution containing 2.5 mg/ml collagenase type IV (Worthington Biochemical, Lakewood, NJ) and 2 mg/ml elastase (Worthington Biochemical) was injected under the epithelial layers of the tongue and palate. The palate was excised immediately after the enzyme injection, and placed into PBS. After 15 min enzyme treatment at room temperature, the tongue and palate were fixed in 4% paraformaldehyde (PFA) in

PBS at 4˚C for 30 min. The epithelium of the tongue and palate was peeled off in PBS and immersed again in 4% PFA in PBS at 4˚C for 15 min. The peeled epithelium was washed 3 times with PBS for 15 min each, and immersed in methanol at -25˚C for 20 min. After washing with TBST (Tris-buffered saline [TBS] containing 0.05% Tween 20), the epithelium was incubated in 10 mM citrate (pH6.0) at 105˚C for 1 min using an electric pressure cooker (EL-MB30, Zojirushi Corp., Osaka, Japan) for antigen retrieval and then cooled to room temperature for about 25 min. The epithelium of the tip of the tongue, circumvallate papillae, and soft palate was trimmed in TBST after antigen retrieval, washed 3 times with TBST for 10 min each and used for immunohistochemistry.

Whole-mount immunohistochemistry and image processing

The peeled epithelium was incubated in TBSB (TBS containing 10% normal donkey serum and 0.3% Triton X-100) for 2 hr at room temperature to block nonspecific staining and incubated with primary antibodies diluted in TBSB overnight at 4 ˚C (Table 1). Control samples were incubated with TBSB without primary antibodies. The tissues were washed 4 times with TBST for 10 min each and incubated with secondary antibodies in TBSB overnight at 4 ˚C (Table 2). The tissues were washed 4 times with TBST containing DAPI (NucBlue, Invitrogen, Carlsbad, CA). The tissues were rinsed with TE (10 mM Tris-HCl (pH8.0), 1 mM EDTA), mounted and coverslipped with Prolong Glass (Invitrogen). Immunofluorescence was imaged on a Leica TCS SP8 confocal microscope equipped with HyD detectors using a 63x/1.4 oil immersion lens. A series of optical sections was acquired at 0.5-0.8 µm intervals from the bottom to the apical portion of the taste buds.

Three-dimensional images were reconstructed from z-stack and resliced using Imaris software (Bitplane, Switzerland). For 3D visualization on Imaris software, “volume” was used in the “normal shading” mode for opaque visualization of IP3R3 and CA4 double color images and in the “blend” mode for semi-transparent visualization of IP3R3, CA4, and NCAM triple color images. Resliced

images were generated using the “oblique slicer” tool. Brightness and contrast were adjusted by Adobe Photoshop (Adobe Systems, San Jose, CA).

Cell counting and statistical analysis

IP3R3(+), CA4(+), and NCAM(+) cells in each taste buds were quantified by confirming the cell shape and nuclear profile in the original z-series optical sections in serial order using the “cell counter” plugin of Fiji/ImageJ (Schindelin et al. 2012).

IBM SPSS Statistics 26 (IBM, New York, NY) and the statistical software R (version 3.6.2; https://www.R-project.org/) were employed for statistical analysis. Parametric data are presented as means ± SD and were analyzed by one-way ANOVA with post hoc Bonferroni test. Non-parametric data were presented in box-dot plots and analyzed by the Mann-Whitney U test. A statistically significant level was set at $p < 0.05$. Scatter plots and histograms were generated with IBM SPSS and area proportional Venn diagrams of colocalization of immunoreactivities were drawn using the “nVennR” package (Pérez-Silva et al. 2018) for R. Box-dot plots were drawn using KaleidaGraph (Synergy Software, Reading, PA).

Results

Expression of IP3R3 and CA4

IP3R3(+) and CA4(+) cells in individual taste buds of the soft palate (SP), fungiform (FF), and circumvallate (CV) papillae were analyzed by whole-mount immunohistochemistry. Signals for IP3R3 and CA4 were clearly detected and segregated completely from each other in all taste buds examined (SP, 233 taste buds; FF, 123; CV, 281) supporting that each is a reliable cell-type-specific marker for Type II or Type III cell, respectively (Figure 1). The signal for IP3R3 was detected throughout the cytoplasm of labeled cells. The CA4 signal was more localized to the cell membrane compared to that for IP3R3. The z-stack serial images enabled us to generate the 3D-reconstruction of whole taste buds from the bottom to the top.

Type II/III cell composition in taste buds

To compare type II/III cell composition in individual taste buds between the SP, FF and CV, IP3R3(+) and CA4(+) cells were enumerated (Figure 2). The mean number of IP3R3(+) cells per taste bud was largest in the SP (22.5 ± 7.3), followed by the FF (12.5 ± 3.6) and CV (10 ± 3.6). In contrast, the largest number of CA4(+) cells per taste bud occurred in the CV (5.9 ± 2.3), followed by the SP (3.6 ± 1.8) and FF (1.7 ± 1.1) (Figure 2). Mean numbers of both IP3R3(+) and CA4(+) cells per taste bud significantly differed between the SP, FF, and CV [IP3R3(+) cells: ANOVA; $F_{(2, 634)} = 381.920$; $P < 0.0001$, post-hoc Bonferroni test; $P < 0.0001$][CA4(+) cells: ANOVA; $F_{(2, 634)} = 219.659$; $P < 0.0001$, post-hoc Bonferroni test; $P < 0.0001$]. Scatter plots were generated to assess the relationship of the number of IP3R3(+) and CA4(+) cells in individual taste buds in each region, and Pearson correlation coefficients were calculated. The numbers of IP3R3(+) and CA4(+) cells per taste bud were moderately correlated in the CV (r = 0.442, $P < 0.001$). However, the correlation was low in the SP (r = 0.279, $P < 0.001$), and no significant correlation was found in the FF (r = -0.011, $P = 0.903$) (Fig. 2).

NCAM expression

NCAM was considered as one of the most reliable Type III cell markers in CV taste buds (Nelson and Finger 1993; Yee et al. 2001), but was not sufficiently investigated in the SP and FF. NCAM expression was examined by three-color detection with IP3R3 and CA4 in the SP, FF, and CV. NCAM immunoreactivity was observed mainly in CA4(+) cells in all three regions. No IP3R3(+) cells were NCAM positive in the CV (Figure S1). However, in the SP (Figure 3) and FF (Figure 4), NCAM immunoreactivity was also detected in subsets of IP3R3(+) cells. IP3R3(+) cells with NCAM were negative for CA4, which is consistent with the evidence that immunoreactivities of IP3R3 and CA4 were completely separated from each other (Figure 1). NCAM signals of the taste cell surface were able to be discriminated from that of the nerves since whole-mount immunohistochemistry visualized cell shape.

NCAM(+) cells not expressing either CA4 or IP3R3 were noted in all regions of SP, FF, and CV (arrows in Figure 5). In the FF, only three cells were identified as this type among 106 NCAM(+) cells observed. These three cells resided in the basal side of the taste buds, and the cell processes were incomplete and did not reach the taste pore (Figure 6). In the SP and CV, most of the NCAM(+) cells without either CA4 or IP3R3 were elongate cells.

Colocalization relationships of IP3R3, CA4 and NCAM, and distribution of NCAM(+)CA(-) cells

Table 3 summarizes the result of the triple immunohistochemistry for IP3R3, CA4, and NCAM in the CV, SP, and FF. The proportion of the subpopulations of taste bud cells identified by immunoreactivities is illustrated by the area proportional Venn diagrams for each region (Figure 7**a**).

In the CV, taste bud cells fell into two cell populations, IP3R3(+) cells and NCAM(+) cells (Figure 7**a**). While NCAM and CA4 are both considered as Type III cell markers, they did not overlap completely. CA4(+) cell population was included in the NCAM(+) cell population, and 11.4% (90/791) of NCAM(+) cells were CA4-negative :NCAM(+)CA4(-) cells (green in Figure 7**a**, CV). In the SP and FF, the CA4(+) cell population was also substantially included in the NCAM(+) cell population, but with a few exceptions [CA4(+)NCAM(-) cells: blue in Figure 7**a**, SP and FF]. The proportion of NCAM(+)CA4(-) cells in NCAM(+) cells in the SP was 22.2% (76/333), which was about twice that in the CV, while it was 8.5% (9/106) in the FF. In contrast to the CV, the majority of NCAM(+)CA(-) cells were unexpectedly IP3R3-positive in the SP (83%: 63/76) and FF (67%: 6/9): IP3R3(+)NCAM(+) cells (yellow in Figure 7**a**). The percentage of IP3R3(+)NCAM(+) cells (yellow) in IP3R3(+) cells was 4.4% (63/1430) in the SP, while it was rare and 0.8% (6/710) in the FF.

To assess the distribution of NCAM(+)CA4(-) cells including IP3R3(+)NCAM(+) cells among taste buds (green or yellow in Figure 7**a**), we divided the taste buds into two groups [taste bud

category #1 (TB#1), taste buds without NCAM(+)CA4(-) cells; taste bud category #2 (TB#2), taste buds with NCAM(+)CA4(-) cells], and created the stacked column chart of the cells belonging to respective subpopulations shown in Figure 7**a** for TB#1 and TB#2 in each region (Figure 7**b-b"**). NCAM(+)CA4(-) cells (green or yellow) were found in 53.3% (65/122), 60.0% (42/70), and 13.8% (8/58) of taste buds examined in the CV, SP, and FF, respectively. The number of NCAM(+)CA4(-) cells per taste bud in TB#2 were 1 to 3, 1 to 4, 1 and 2 in the CV, SP, and FF, respectively. Assuming the total number of taste cells counted in the respective taste buds in the immunohistochemistry reflects the size of the taste buds, the size of taste buds containing NCAM(+)CA4(-) cells (TB#2 in Figure 7**b-b"**) varied over the entire range, and there was no obvious correlation between the occurrence of NCAM(+)CA4(-) cells and the size of taste buds in TB#2 in any regions.

Quantitative relationships between NCAM(+)CA4(-) cells and other cells in the taste buds

Does the occurrence of NCAM(+)CA4(-) cells change the abundance of other cells in taste buds? To investigate how the occurrence of NCAM(+)CA4(-) cells influences the abundance of other cells in the taste buds, we generated box-dot plots and compared the number of CA4(+), NCAM(+), and IP3R3(+) cells, and total counts of these cells per taste bud between TB#1 and TB#2 (Figure 7**c**).

In the CV, there were no differences in the number of CA4(+) cells between TB#1 and TB#2 (Figure 7**c**). The number of NCAM(+) cells per taste bud was significantly larger in TB#2 than in TB#1, indicating that, in the NCAM(+) cell population, NCAM(+)CA4(-) cells (green in Figure 7**b**, CV) may be simply added to CA4(+) cells in TB#2. The number of IP3R3(+) cells , which are identical to IP3R3(+)NCAM(-) cells in the CV since no IP3R3(+)NCAM(+) cells (yellow) exist, was not different between TB#1 and TB#2 in the CV. Reflecting the larger number of NCAM(+) cells in TB#2, there was a tendency for the total cell counts to be larger in TB#2 than in TB#1, while there was no statistically-significant difference (Figure 7**c**).

In the SP and FF, no difference was found in the number of CA4(+) cells between TB#1 and TB#2. The number of NCAM(+) cells showed a tendency to be greater in TB#2 than in TB#1, while the statistical significance was found only in the SP. Statistically significant differences were found in IP3R3(+) cells, which include IP3R3(+)NCAM(+) cells (yellow in Figure 7**b'b"**, SP and FF), but no differences were found in IP3R3(+)NCAM(-) cells similar to that in the CV. The total cell counts tended to be larger in TB#2 than in TB#1, while statistical significance was detected only in the FF.

In summary, in all taste regions, the number of cells showed tendencies to be grater in TB#2 than in TB#1 when the cells included NCAM(+)CA(-) cells, and no differences were found when the cells did not include NCAM(+)CA4(-) cells.

Discussion

Diversity of Type II/III cell composition among taste buds

We examined taste buds by whole-mount immunohistochemistry to enumerate precisely IP3R3(+) and CA4(+) cells in individual taste buds in the CV, FF, and SP. CA4 was previously shown to be segregated from PLCβ2 and TrpM5, key molecules of Ca^{2+} signaling specific to Type II cells (Lossow et al. 2017). Here, we showed CA4 never overlaps with IP3R3, which is indispensable for signal transduction from PLCβ2 to TrpM5 in Type II cells (Hisatsune et al. 2007). Our results corroborated the reliability of these markers and also showed that the ratio between Type II and III cells in each taste bud varied widely among taste buds in respective taste regions (Pearson's r =0.442 [CV], 0.279 [SP], and -0.011[FF]) (Figure 2).

It was generally assumed that the three respective types of taste cells are housed in proper ratios in each taste bud (Ma et al. 2007; Ohtubo and Yoshii 2011; Barlow and Klein 2015; Roper and Chaudhari 2017; Ogata and Ohtubo 2020). Type I cells are most abundant and approximately half of the cells in a taste bud. Type II cells are approximately one-third, and Type III cells are least frequent and 2-20% (Roper and Chaudhari 2017). The occurrence of Type III cells is dependent on

the specific taste regions, i.e. more frequent in the CV than in the FF (Ma et al. 2007; Ohtubo and Yoshii 2011). Several studies have assessed Type II and III cell contents in respective taste buds (Ma et al. 2007; Miura et al. 2007; Ohtubo and Yoshii 2011; Ogata and Ohtubo 2020) and revealed regional differences. Recently, Ogata and Ohtubo (2020) reported from whole-mount immunohistochemistry using IP3R3 and PLCβ2 as Type II markers and SNAP-25 as a Type III marker that Type II cells were approximately 25% of taste bud cells regardless of the taste region and that Type III in the CV and FL were approximately 11%, which was approximately twice higher than that in the FF and SP. They assessed the correlation between the number of Type II or III cells versus taste bud size and concluded that the number of each cell type per taste bud is proportional to the size of taste buds (Ohtubo and Yoshii 2011; Ogata and Ohtubo 2020). However, the correlation of the cell numbers between Type II and III cells in the respective taste buds was not directly assessed. The concept that each taste bud contains a ratio of taste cells in the order of Type I, II, and III depending on the taste regions has not been carefully explored. Our data here illuminated the vast diversity of Type II/III cell composition among taste buds. The respective types of cells were housed in individual taste buds rather independently.

Cell type differentiation from stem/progenitor cells

The idea of a proper ratio of cell types in each taste bud is likely associated with a simple deterministic model of cell differentiation (Theise and Harris 2006). However, the vast diversity of Type II/III cell composition in the present results suggest that cell type differentiation occurs more stochastically than previously assumed in the taste buds. Recent studies demonstrate that Type II and III cell differentiation is altered by various signaling pathways in the taste bud stem/progenitor cell niche.

Lgr5(+) and Lgr6(+) cells were reported as taste bud stem/progenitor cells (Takeda et al. 2013; Yee et al. 2013; Ren et al. 2014). β-Catenin stabilization, a key step in Wnt signaling in keratin5(+) stem/progenitor cells using an inducible Cre-loxP system increased Type II cells but not Type III

cells, while cell type expansion occurred more remarkably in Type I cells (Gaillard and Barlow 2011; Gaillard et al. 2015). The difference in Wnt signaling between taste buds may cause cell-type diversity through the stabilization of β-Catenin, especially in the FF and SP, where every taste bud possesses more Type II than Type III cells.

Ren and colleagues (2014) demonstrated that single Lgr5(+) or Lgr6(+) cells could give rise to all taste cell types, Type I, II, and III, in organoid cultures. Wnt, Bone Morphogenetic Protein (BMP), Hedgehog (Hh), and Notch signaling were shown to have a great impact on the growth and differentiation of taste organoids (Ren et al. 2017). The conditional knockout of Gli3, a suppressor of Hh signaling, in the Lgr5(+) cells increased Type II cells but not Type III cells in taste organoids (Qin et al. 2018). Hh signaling from basal cells of taste buds and taste nerves was also shown to be critical for taste cell development (Miura et al. 2001; Castillo-Azofeifa et al. 2017). The difference in Hh signaling between taste buds may also cause cell type diversity. It may also be noteworthy that multiple cell type differentiation was not always observed in organoid cell clusters (Ren et al. 2014). This seems to reflect the intrinsic nature of stem/progenitor cells in which cell fate can be easily altered by a slight change in microenvironment of stem cell niche.

The number of progenitor cells that contribute to an average size-taste bud in the CV was estimated to be at least eight based on the analysis of X chromosome-inactivation mosaic mice (Stone et al. 2002). The assembly of stem/progenitor cells with a distinct differentiation potential may further increase the diversity of cell-type composition within taste buds.

Identity of NCAM(+)CA4(-) cells as a cell type found only in a subset of taste buds

We found that NCAM(+)CA(-) cells occur in a subset of taste buds, independently from the spatial location and size of taste buds (Figure 7**b-b”**). The occurrence of these cells in TB#2 was simply additive when cell numbers were compared between TB#1 and TB#2 and did not decrease the abundance of cells of other types in TB#2 (Figure 7**c**).

We previously proposed that Type II cells are derived from *Mash*-expressing cells, which are NCAM(+), based on expression analysis during taste bud development in the CV by using the combination of immunohistochemistry of NCAM and *in situ* hybridization of *Mash1*, *Gα-gust*, and *T1r3* (Kusakabe et al. 2002; Miura et al. 2005, 2006). We found ~10% of the cells expressing mRNA of *Gα-gust* or *T1r3*, Type II cell-specific genes, were NCAM(+) in adult mice, while immunohistochemical signals for NCAM and Gα-gust did not overlap. Temporal changes of NCAM immunoreactivity during taste bud development supported that NCAM immunoreactivity in *Gα-gust* and *T1r3*-expressing cells is a remnant from the *Mash1*-expressing stage and is down-regulated during the maturation of taste cells. Recently reported was that 34.6% (255/737) of PLCβ2(+) Type II CV cells were tdTomato-positive after a two-day continuous Tamoxifen treatment of Ascl1^{CreERT2} CAG-floxed tdTomato mice, proving that *Mash1*-expressing cells indeed give rise to Type II cells (Hsu et al. 2020).

Based on the idea that Type II cells, if not all, are derived from *Mash*-expressing NCAM(+) cells in the CV, NCAM(+)CA4(-) cells in the CV in the present study, which were IP3R3(-), appear to be mainly composed of the immature Type II cells possessing remnant NCAM immunoreactivity. Assuming the NCAM(+)CA4(-)IP3R3(-) cells are immature Type II cells and express mRNA of Type II cell-specific genes, the percentage of NCAM(+) cells in taste cells expressing Type II cell-specific genes is 7.1% [90/(90+1183), NCAM(+)CA4(-) cells/(NCAM(+)CA4(-) cells + IP3R3(+) cells)]. This percentage is likely comparable to that previously reported (~10%) (Miura et al. 2005), while the previous data (~10%) might be slightly overestimated because of the lower histochemical resolution of the combination of immunohistochemistry and *in situ* hybridization compared to the resolution of whole-mount immunohistochemistry employed in this study. To assess if NCAM(+)CA4(-) cells are immature cells, further lineage tracing studies are needed using BrdU/EdU tracing or lineage analysis like using Ascl1^{CreERT2} mice (Hsu et al. 2020) in combination with NCAM and CA4 immunohistochemistry.

On the other hand, in the SP and FF, the majority of NCAM(+)CA4(-) cells were IP3R3(+) different from that in the CV. If these cells are immature cells of Type II cell lineage similar to that supposed in the CV, NCAM expression should be downregulated during cell maturation. In this case, the time course of NCAM protein expression differed between CV and SP/FF during Type II cell maturation. We previously reported that cell differentiation within taste bud primordia in mouse embryos progress much faster in the SP than in other regions (Harada et al. 2000; Nakayama et al. 2015). The difference in cell differentiation may continue in cell turnover in adult taste buds causing a difference in the NCAM protein expression. We cannot rule out the possibility that NCAM(+)IP3R3(+) cells are mature and represent a unique subpopulation of taste cells. Further studies are needed to reveal the cell identity of NCAM(+)IP3R3(+) cells.

Conclusions

In the present study, we demonstrated that Type II and III cells are housed almost independently in respective taste buds. The vast diversity of Type II/III cell composition among taste buds reflects the property of stem/progenitor cells for taste buds. While the reliability of CA4 as a Type III cell marker was confirmed, NCAM immunoreactivity was observed in IP3R3(+) cells in the SP and FF. The characterization of NCAM(+)IP3R3(+) cells will require further investigation.

Taste buds are generally assumed to be composed of different cell types in a particular ratio corresponding to taste regions. Our findings shed light on the heterogeneity of taste buds in each taste region and suggest more dynamic changes in size and cell composition of taste buds during cell turnover than previously appreciated. The consistency of gustatory function is maintained on the summation of such dynamic cell kinetics in taste buds.

Acknowledgements

The authors thank Dr. Ayumi Nakayama for technical support for whole mount immunohistochemistry and Dr. John Caprio for valuable comments on the manuscript.

Declarations

Funding

This work was supported by Japan Society for the Promotion of Science (JSPS) KAKENHI Grant Numbers JP17K11647 and JP20K09892 to HM.

Conflicts of Interest

The authors state that there is no conflict of interest.

Ethical approval

All experimental procedures were approved by the institutional animal care and use committees and were conducted at Kagoshima University.

References

Bachmanov AA, Beauchamp GK, Tordoff MG (2002) Voluntary consumption of NaCl, KCl, CaCl2, and NH4Cl solutions by 28 mouse strains. Behav Genet 32:445–457. https://doi.org/10.1023/A:1020832327983

Banik DD, Benfey ED, Martin LE, et al (2020) A subset of broadly responsive Type III taste cells contribute to the detection of bitter, sweet and umami stimuli. PLOS Genet 16:e1008925. https://doi.org/10.1371/journal.pgen.1008925

Barlow LA, Klein OD (2015) Developing and Regenerating a Sense of Taste. In: Curr Top Dev Biol. pp 401–419. https://doi.org/10.1016/bs.ctdb.2014.11.012

Barlow LA, Northcutt RG (1995) Embryonic Origin of Amphibian Taste Buds. Dev Biol 169:273–285. https://doi.org/10.1006/dbio.1995.1143

Bartel DL, Sullivan SL, Lavoie ÉG, et al (2006) Nucleoside triphosphate diphosphohydrolase-2 is the ecto-ATPase of type I cells in taste buds. J Comp Neurol 497:1–12. https://doi.org/10.1002/cne.20954

Baumer-Harrison C, Raymond MA, Myers TA, et al (2020) Optogenetic stimulation of type I GAD651 cells in taste buds activates gustatory neurons and drives appetitive licking behavior in sodium-depleted mice. J Neurosci 40:7795–7810. https://doi.org/10.1523/JNEUROSCI.0597-20.2020

Beidler LM, Smallman RL (1965) Renewal of cells within taste buds. J Cell Biol 27:263–272. https://doi.org/10.1083/jcb.27.2.263

Castillo-Azofeifa D, Losacco JT, Salcedo E, et al (2017) Sonic hedgehog from both nerves and epithelium is a key trophic factor for taste bud maintenance. Development 144:3054–3065. https://doi.org/10.1242/dev.150342

Chandrashekar J, Kuhn C, Oka Y, et al (2010) The cells and peripheral representation of sodium taste in mice. Nature 464:297–301. https://doi.org/10.1038/nature08783

Chandrashekar J, Yarmolinsky D, von Buchholtz L, et al (2009) The taste of carbonation. Science (80-) 326:443–445. https://doi.org/10.1126/science.1174601

Chaudhari N, Roper SD (2010) The cell biology of taste. J Cell Biol 190:285–296. https://doi.org/10.1083/jcb.201003144

Clapp TR, Medler KF, Damak S, et al (2006) Mouse taste cells with G protein-coupled taste receptors lack voltage-gated calcium channels and SNAP-25. BMC Biol 4:1–9. https://doi.org/10.1186/1741-7007-4-7

DeFazio RA, Dvoryanchikov G, Maruyama Y, et al (2006) Separate populations of receptor cells and presynaptic cells in mouse taste buds. J Neurosci 26:3971–3980. https://doi.org/10.1523/JNEUROSCI.0515-06.2006

Dvoryanchikov G, Huang YA, Barro-Soria R, et al (2011) GABA, Its Receptors, and GABAergic Inhibition in Mouse Taste Buds. J Neurosci 31:5782–5791. https://doi.org/10.1523/JNEUROSCI.5559-10.2011

Dvoryanchikov G, Tomchik SM, Chaudhari N (2007) Biogenic amine synthesis and uptake in rodent taste buds. J Comp Neurol 505:302–313. https://doi.org/10.1002/cne.21494

Farbman AI (1980) RENEWAL OF TASTE BUD CELLS IN RAT CIRCUMVALLATE PAPILLAE. Cell Prolif. https://doi.org/10.1111/j.1365-2184.1980.tb00474.x

Finger TE, Danilova V, Barrows J, et al (2005) Neuroscience: ATP signaling is crucial for communication from taste buds to gustatory nerves. Science 310:1495–1499. https://doi.org/10.1126/science.1118435

Finger TE, Simon SA (2000) Cell biology of taste epithelium. In: Finger TE, Silver WL, Restrepo D (eds) The Neurobiology of Taste and Smell, Second. Wiley-Liss, New York, pp 287–314

Gaillard D, Barlow LA (2011) Taste bud cells of adult mice are responsive to Wnt/β-catenin signaling: Implications for the renewal of mature taste cells. Genesis 49:295–306. https://doi.org/10.1002/dvg.20731

Gaillard D, Xu M, Liu F, et al (2015) β-Catenin Signaling Biases Multipotent Lingual Epithelial Progenitors to Differentiate and Acquire Specific Taste Cell Fates. PLoS Genet 11. https://doi.org/10.1371/journal.pgen.1005208

Harada S, Yamaguchi K, Kanemaru N, Kasahara Y (2000) Maturation of taste buds on the soft palate of the postnatal rat. Physiol Behav 68:333–339. https://doi.org/10.1016/S0031-9384(99)00184-5

Hisatsune C, Yasumatsu K, Takahashi-Iwanaga H, et al (2007) Abnormal Taste Perception in Mice Lacking the Type 3 Inositol 1,4,5-Trisphosphate Receptor. J Biol Chem 282:37225–37231. https://doi.org/10.1074/jbc.M705641200

Hsu CC, Seta Y, Matsuyama K, et al (2020) Mash1-expressing cells may be relevant to type III cells and a subset of PLCβ2-positive cell differentiation in adult mouse taste buds. Cell Tissue Res. https://doi.org/10.1007/s00441-020-03283-w

Huang AL, Chen X, Hoon MA, et al (2006) The cells and logic for mammalian sour taste detection. Nature 442:934–938. https://doi.org/10.1038/nature05084

Ishimaru Y, Inada H, Kubota M, et al (2006) Transient receptor potential family members PKD1L3 and PKD2L1 form a candidate sour taste receptor. Proc Natl Acad Sci U S A 103:12569–12574. https://doi.org/10.1073/pnas.0602702103

Kataoka S, Yang R, Ishimaru Y, et al (2008) The candidate sour taste receptor, PKD2L1, Is expressed by type III taste cells in the mouse. Chem Senses 33:243–254. https://doi.org/10.1093/chemse/bjm083

Kim D -J, Roper SD (1995) Localization of serotonin in taste buds: A comparative study in four vertebrates. J Comp Neurol. https://doi.org/10.1002/cne.903530304

Kinnamon SC, Finger TE (2019) Recent advances in taste transduction and signaling. F1000Research 8:2117. https://doi.org/10.12688/f1000research.21099.1

Kusakabe Y, Miura H, Hashimoto R, et al (2002) The Neural Differentiation Gene Mash-1 has a Distinct Pattern of Expression from the Taste Reception-related Genes gustducin and T1R2 in the Taste Buds. Chem Senses 27:445–451. https://doi.org/10.1093/chemse/27.5.445

Lossow K, Hermans-Borgmeyer I, Behrens M, Meyerhof W (2017) Genetic labeling of Car4-expressing cells reveals subpopulations of type III taste cells. Chem Senses 42:747–758. https://doi.org/10.1093/chemse/bjx048

Ma H, Yang R, Thomas SM, Kinnamon JC (2007) Qualitative and quantitative differences between taste buds of the rat and mouse. BMC Neurosci 8:1–13. https://doi.org/10.1186/1471-2202-8-5

Ma Z, Taruno A, Ohmoto M, et al (2018) CALHM3 Is Essential for Rapid Ion Channel-Mediated Purinergic Neurotransmission of GPCR-Mediated Tastes. Neuron 98:547-561.e10. https://doi.org/10.1016/j.neuron.2018.03.043

Miura H, Kato H, Kusakabe Y, et al (2005) Temporal changes in NCAM immunoreactivity during taste cell differentiation and cell lineage relationships in taste buds. Chem Senses 30:367–375. https://doi.org/10.1093/chemse/bji031

Miura H, Kusakabe Y, Harada S (2006) Cell lineage and differentiation in taste buds. Arch Histol Cytol 69:209–225. https://doi.org/10.1679/aohc.69.209

Miura H, Kusakabe Y, Hashido K, et al (2014a) The glossopharyngeal nerve controls epithelial expression of Sprr2a and Krt13 around taste buds in the circumvallate papilla. Neurosci Lett 580:147–152. https://doi.org/10.1016/j.neulet.2014.08.012

Miura H, Kusakabe Y, Sugiyama C, et al (2001) Shh and Ptc are associated with taste bud maintenance in the adult mouse. Mech Dev 106: 143–145. https://doi.org/10.1016/S0925-4773(01)00414-2

Miura H, Nakayama A, Shindo Y, et al (2007) Expression of gustducin overlaps with that of type III IP3 receptor in taste buds of the rat soft palate. Chem Senses 32:689–696. https://doi.org/10.1093/chemse/bjm036

Miura H, Scott JK, Harada S, Barlow LA (2014b) Sonic hedgehog-expressing basal cells are general post-mitotic precursors of functional taste receptor cells. Dev Dyn 243:1286–1297. https://doi.org/10.1002/dvdy.24121

Nakayama A, Miura H, Ooki M, Harada S (2015) During development intense Sox2 expression marks not only Prox1-expressing taste bud cell but also perigemmal cell lineages. Cell Tissue Res 359:743–753. https://doi.org/10.1007/s00441-014-2076-5

Nelson GM, Finger TE (1993) Immunolocalization of different forms of neural cell adhesion molecule (NCAM) in rat taste buds. J Comp Neurol 336:507–516. https://doi.org/10.1002/cne.903360404

Ogata T, Ohtubo Y (2020) Quantitative Analysis of Taste Bud Cell Numbers in the Circumvallate and Foliate Taste Buds of Mice. Chem Senses. https://doi.org/10.1093/chemse/bjaa017

Ohtubo Y, Yoshii K (2011) Quantitative analysis of taste bud cell numbers in fungiform and soft palate taste buds of mice. Brain Res 1367:13–21. https://doi.org/10.1016/j.brainres.2010.10.060

Oka Y, Butnaru M, von Buchholtz L, et al (2013) High salt recruits aversive taste pathways. Nature 494:472–475. https://doi.org/10.1038/nature11905

Okubo T, Clark C, Hogan BLM (2009) Cell Lineage Mapping of Taste Bud Cells and Keratinocytes in the Mouse Tongue and Soft Palate. Stem Cells 27:442–450. https://doi.org/10.1634/stemcells.2008-0611

Pérez-Silva JG, Araujo-Voces M, Quesada V (2018) nVenn: generalized, quasi-proportional Venn and Euler diagrams. Bioinformatics 34:2322–2324. https://doi.org/10.1093/bioinformatics/bty109

Qin Y, Sukumaran SK, Jyotaki M, et al (2018) Gli3 is a negative regulator of Tas1r3-expressing taste cells. PLOS Genet 14:e1007058. https://doi.org/10.1371/journal.pgen.1007058

Ren W, Aihara E, Lei W, et al (2017) Transcriptome analyses of taste organoids reveal multiple pathways involved in taste cell generation. Sci Rep 7:4004. https://doi.org/10.1038/s41598-017-04099-5

Ren W, Lewandowski BC, Watson J, et al (2014) Single Lgr5- or Lgr6-expressing taste stem/progenitor cells generate taste bud cells ex vivo. Proc Natl Acad Sci 111:16401–16406. https://doi.org/10.1073/pnas.1409064111

Roper SD, Chaudhari N (2017) Taste buds: Cells, signals and synapses. Nat Rev Neurosci 18:485–497. https://doi.org/10.1038/nrn.2017.68

Schindelin J, Arganda-Carreras I, Frise E, et al (2012) Fiji: an open-source platform for biological-image analysis. Nat Methods 9:676–682. https://doi.org/10.1038/nmeth.2019

Shigemura N, Ninomiya Y (2016) Recent Advances in Molecular Mechanisms of Taste Signaling and Modifying. Int Rev Cell Mol Biol 323:71-106. https://doi.org/10.1016/bs.ircmb.2015.12.004

Stone LM, Finger TE, Tam PPL, Tan SS (1995) Taste receptor cells arise from local epithelium, not neurogenic ectoderm. Proc Natl Acad Sci U S A 92:1916–1920. https://doi.org/10.1073/pnas.92.6.1916

Stone LM, Tan SS, Tam PPL, Finger TE (2002) Analysis of Cell Lineage Relationships in Taste Buds. J Neurosci 22:4522–4529. https://doi.org/10.1523/jneurosci.22-11-04522.2002

Sukumaran SK, Lewandowski BC, Qin Y, et al (2017) Whole transcriptome profiling of taste bud cells. Sci Rep 7:1–15. https://doi.org/10.1038/s41598-017-07746-z

Takeda M, Suzuki Y, Obara N, Nagai Y (1992) Neural cell adhesion molecule of taste buds. J Electron Microsc (Tokyo). https://doi.org/10.1093/oxfordjournals.jmicro.a050981

Takeda N, Jain R, Li D, et al (2013) Lgr5 Identifies Progenitor Cells Capable of Taste Bud Regeneration after Injury. PLoS One 8:1–8. https://doi.org/10.1371/journal.pone.0066314

Taruno A, Vingtdeux V, Ohmoto M, et al (2013) CALHM1 ion channel mediates purinergic neurotransmission of sweet, bitter and umami tastes. Nature 495:223–226. https://doi.org/10.1038/nature11906

Theise ND, Harris R (2006) Postmodern biology: (Adult) (stem) cells are plastic, stochastic, complex, and uncertain. Handb Exp Pharmacol 174:389–408. https://doi.org/10.1007/3-540-31265-X-16

Tomchik SM, Berg S, Joung WK, et al (2007) Breadth of tuning and taste coding in mammalian taste buds. J Neurosci 27:10840–10848. https://doi.org/10.1523/JNEUROSCI.1863-07.2007

Wilson CE, Finger TE, Kinnamon SC (2017) Type III cells in anterior taste fields are more immunohistochemically diverse than those of posterior taste fields in mice. Chem Senses 42:759–767. https://doi.org/10.1093/chemse/bjx055

Yang R, Crowley HH, Rock ME, Kinnamon JC (2000) Taste cells with synapses in rat circumvallate papillae display SNAP-25-like immunoreactivity. J Comp Neurol 424:205–215. https://doi.org/10.1002/1096-9861(20000821)424:2<205::AID-CNE2>3.0.CO;2-F

Yee CL, Yang R, Böttger B, et al (2001) "Type III" cells of rat taste buds: Immunohistochemical and ultrastructural studies of neuron-specific enolase, protein gene product 9.5, and serotonin. J Comp Neurol 440:97–108. https://doi.org/10.1002/cne.1372

Yee KK, Li Y, Redding KM, et al (2013) Tissue - specific stem cells Lgr5-EGFP Marks Taste Bud Stem / Progenitor Cells. Stem Cells 31:992–1000. https://doi.org/10.1002/ber

Table 1. Primary antibodies

Target	Host	Dilution	Manufacturer	Cat No.	RRID	Lot
NCAM	Rabbit	1:200	Millipore (Temecula, CA)	AB5032	AB_2291692	JC1658210
IP3R3	Mouse	1:100	BD Biosciences (San Jose, CA)	610313	AB_397705	7173977
CA4	Goat	1:100	R&D systems (Minneapolis, MN)	AF2414	AB_2070332	WKG0111071

Table 2. Secondary antibodies

Target	Host	Dilution	Manufacturer	Cat No.	RRID	Conjugated dye
Rabbit IgG	donkey	1:400	Molecular Probes (Eugene, OR)	A21206	AB_2535792	Alexa Fluor 488
Mouse IgG	donkey	1:400	Molecular Probes (Eugene, OR)	A31570	AB_2536180	Alexa Fluor 555
Goat IgG	donkey	1:400	Molecular Probes (Eugene, OR)	A21082	AB_2535739	Alexa Fluor 633

Table 3. Summary of three-color immunohistochemistry

		IP3R3	NCAM	CA4	Only
SP	IP3R3		4.4%	0%	95.6%
			(63)	ND	(1367)
No. of TB	NCAM*	18.4%		77.8%	3.8%
70		(63)		(267)	(13)
	CA4	0%	98.9%		1.1%
		ND	(267)		(3)
FF	IP3R3		0.8%	0%	99.2%
			(6)	ND	(704)
No. of TB	NCAM*	5.7%		91.5%	2.8%
58		(6)		(97)	(3)
	CA4	0%	97.00%		3.00%
		ND	(97)		(3)
CV	IP3R3		0%	0%	100.0%
			ND	ND	(1183)
No. of TB	NCAM	0%		88.6%	11.4%
122		ND		(701)	(90)
	CA4	0%	100.0%		0%
		ND	(701)		ND

The ratio (%) of taste cells positive for both molecules shown in the top row and left column among the taste cells positive for the molecule in the left column.
"Only" indicates the cells positive only for the molecule shown in the left column but negative for the others.
Numbers in parentheses indicate the total number of cells counted in each category.
ND, not detected.
*: NCAM(+) cell populations in the SP and FF were significantly different according to Chi-square test (P = 0.006974).

Figure Captions

Fig. 1 Expression of IP3R3 (green) and CA4 (magenta) in the taste buds of the SP (**a-d**), FF (**e-h**) and CV (**i-l**). The expression was detected by whole mount immunohistochemistry. The optical section and 3D-projection image (apical view) were obtained from the same taste bud in each region. The signals for IP3R3 and CA4 completely segregated. Scale bar, 10 μm.

Fig. 2 Scatter plots of IP3R3(+) and CA4(+) cell contents in individual taste buds of the CV (**a**), FF (**b**), and SP (**c**). The red color gradient of circles indicates the count of taste buds possessing respective combinations of IP3R3(+) and CA4(+) cells. Pearson's r is shown in the top left of each plot, accompanied by p-value. Linear regression lines are shown for the CV and SP, in which the statistical significance was found. The histogram of taste buds for the number of IP3R3(+) cells in individual taste buds is shown above the scatter plot (**a'**,**b'**,**c'**), and that for CA4(+) cells on the right (**a"**,**b"**,**c"**). The figures in parentheses above the histograms indicate the mean ± SD of the number of IP3R3(+) or CA4(+) cells per taste bud. The table indicates the numbers of taste buds and taste cells counted in the CV, FF and SP.

Fig. 3 Colocalization of IP3R3 and NCAM immunoreactivities in the SP. IP3R3 (red), NCAM (green) and CA4 (blue) were detected by whole mount immunohistochemistry. **a,b-b"** 3D-projection image of the taste bud and resliced sections [(a'),(a")]. The basal side of taste buds to the bottom. **a'**,**a"** The resliced sections are perpendicular each other. In the slice images, the cutting plane of the other resliced section is shown by the white line marked with (a',c-c'") or (a",d-d'"). The signals for nuclei detected by DAPI are shown in gray scale. **c-c'"** The resliced section (**a'**). **d-d'"** The resliced section (**a"**). The arrow indicates the cell expressing both IP3R3 and NCAM. The arrowhead indicates the cells co-expressing NCAM and CA4. Scaler bar, 10 μm.

Fig. 4 Colocalization of IP3R3 and NCAM immunoreactivities in the FF. Legend is same as in Figure 3.

Fig 5 NCAM expression separated from IP3R3 and CA4 expression in the SP (**a**-**d**), FF (**e**-**h**) and CV (**i**-**l**). The arrow indicates the cells positive for NCAM (green) but negative for both IP3R3 (red) and CA4 (blue). The arrowhead indicates the cells co-expressing NCAM and CA4 in the CV. The outlined arrowhead indicates the cells co-expressing IP3R3 and NCAM in the SP. Scale bar, 10 μm.

Fig. 6 3D-projecion image of the taste bud in the FF (**a**-**d**). The arrow indicates an example of the NCAM(+) cell (green) without CA4 (blue) or IP3R3 (red). The arrowhead indicates NCAM(+)CA4(+) cells. The basal side of taste bud to the bottom. Scale bar, 10 μm.

Fig. 7 Quantitative summaries of IP3R3(+), CA4(+), and NCAM(+) cells in the CV, SP, and FF. **a** Area proportional Venn diagrams showing the colocalization relationships of the immunoreactivities for IP3R3, CA4, and NCAM in the taste buds of the CV, SP, and FF. The expression is color-coded in the same RGB color-system as in Figure 3-6: Red, IP3R3; Green, NCAM; Blue, CA4. Yellow (Red + Green) indicates positive for IP3R3 and NCAM but not for CA4. Cyan (Green + Blue) indicates positive for NCAM and CA4 but not for IP3R3 (see the graphical legend at the bottom of Figure 7**a**). IP3R3 and CA4 double-positive cells were not observed in any region. The numeral in the center of each circle indicates the numbers of cells identified in each category, and the area of the circle proportionally indicates the numbers of cells in respective populations in each region. In the CV, taste bud cells are divided into IP3R3(+) and NCAM(+) cell populations. CA4(+) cells are included in the NCAM(+) cell population. In the SP and FF, CA4(+) cells are also virtually included in NCAM(+) cells but with a few exceptions (blue), and the majority of NCAM(+)CA(-) cells are IP3R3(+) (yellow). **b**-**b”** Stacked column chats of the number of immunopositive cells detected in individual taste buds (TB) in the CV (**b**), SP (**b’**), and

FF (**b’’**). The color-coding is the same as in **a**. Taste buds were classified into two categories: TB#1, TBs without NCAM(+)CA4(-) cells (green and yellow), TB#2, TBs with NCAM(+)CA(-) cells. The legend symbol above the graphs, which consists of five small ellipses, is the same as in **a** but reduced. The hatched area in the legend symbol indicates the cells not existing in TB#1. In the stacked column charts, data were arranged in ascending order of total counts of cells per taste bud in TB#1 and TB#2, respectively. The numerals in the chart indicate the number of taste buds counted in TB#1 and TB#2, respectively. In TB#2, no obvious correlation was noted between the occurrence of NCAM(+)CA4(-) cells (green and yellow) and the total counts of cells per taste bud. **c** Comparison of the number of respective cells per taste bud between TB#1 and TB#2. The top row indicates the cells compared: Total cells, CA4(+) cells, NCAM(+) cells, IP3R3(+) cells, and IP3R3(+)NCAM(-) cells. White and black spots indicate TB#1 and TB#2, respectively, and the hatched area indicates the cell populations lacking in TB#1. In the schematic representation, the areas surrounded by bold lines indicate the respective cell populations. The vertical axis in the plots represents the cell counts per taste bud. The numeral on the top of each plot is P value of Mann-Whitney U test. P-values less than 0.05 are shown in red indicating statistically significant differences. General trends in differences between TB#1 and TB#2 seem to be shared between regions. The total number of cells tends to be higher in TB#2 than in TB#1, while the statistically significant difference was detected only in the FF. No differences were found in CA4(+) cells. The number of NCAM(+) cells was higher in TB#2 than in TB#1, while the statistically significant difference was not detected in the FF. The number of IP3R3(+) cells was higher in TB#2 than in TB#1, and no differences were noted in IP3R3(+)NCAM(-) cells between TB#1 and TB#2.

Fig. S1 Stereoscopic views of NCAM(+) and IP3R(+) cells in the CV. The maximum intensity projection images. The cell shape of both NCAM(+) (green) and IP3R3(+) (magenta) cells was clearly observed. Arrows indicate examples of nerve fibers detected by the anti-NCAM antibody. Scale bar, 10 μm.

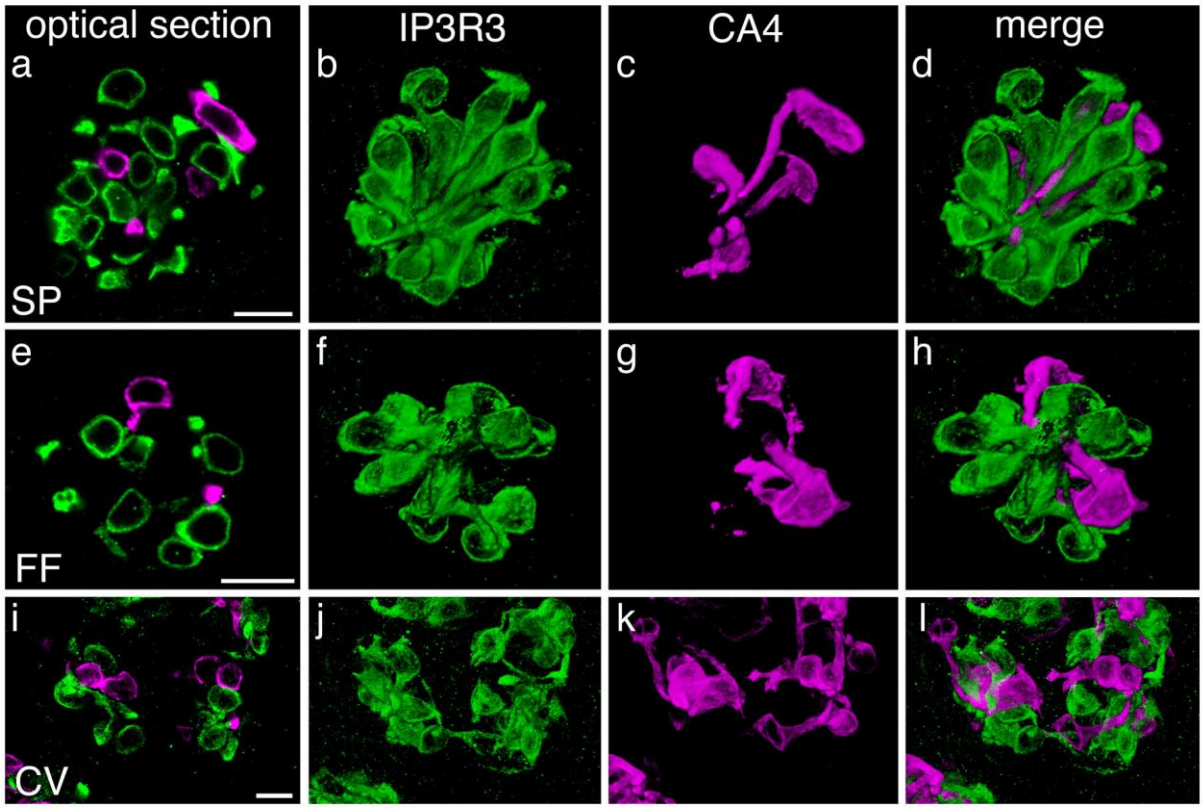

Fig. 1 Expression of IP3R3 (green) and CA4 (magenta) in the taste buds of the SP (**a**-**d**), FF (**e**-**h**) and CV (**i**-**l**). The expression was detected by whole mount immunohistochemistry. The optical section and 3D-projection image (apical view) were obtained from the same taste bud in each region. The signals for IP3R3 and CA4 completely segregated. Scale bar, 10 μm.

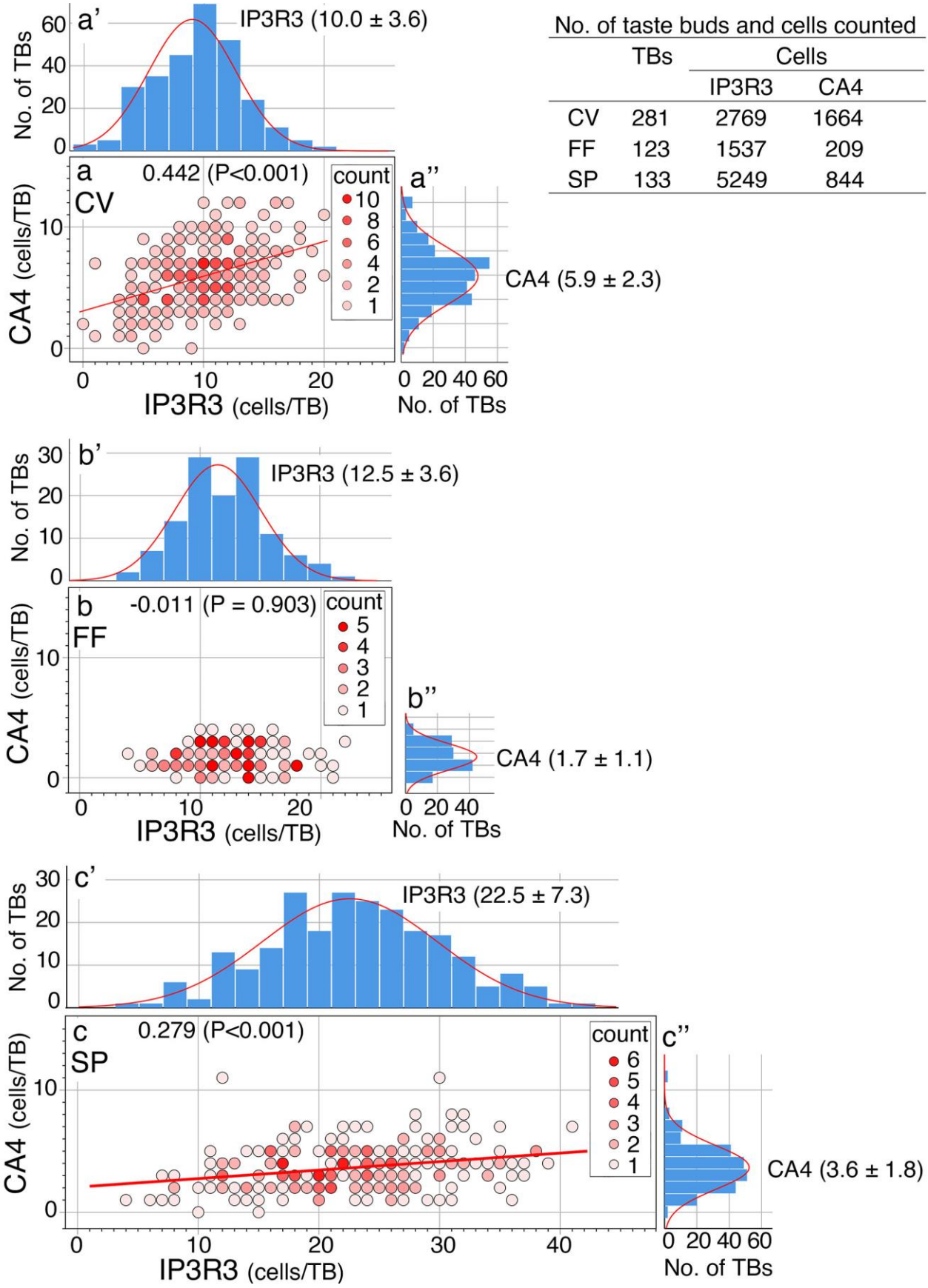

No. of taste buds and cells counted

	TBs	Cells	
		IP3R3	CA4
CV	281	2769	1664
FF	123	1537	209
SP	133	5249	844

Fig. 2 Scatter plots of IP3R3(+) and CA4(+) cell contents in individual taste buds of the CV (**a**), FF (**b**), and SP (**c**). The red color gradient of circles indicates the count of taste buds possessing respective combinations of IP3R3(+) and CA4(+) cells. Pearson's r is shown in the top left of each plot, accompanied by p-value. Linear regression lines are shown for the CV and SP, in which the statistical significance was found. The histogram of taste buds for the number of IP3R3(+) cells in individual taste buds is shown above the scatter plot (**a'**,**b'**,**c'**), and that for CA4(+) cells on the right (**a''**,**b''**,**c''**). The figures in parentheses above the histograms indicate the mean ± SD of the number of IP3R3(+) or CA4(+) cells per

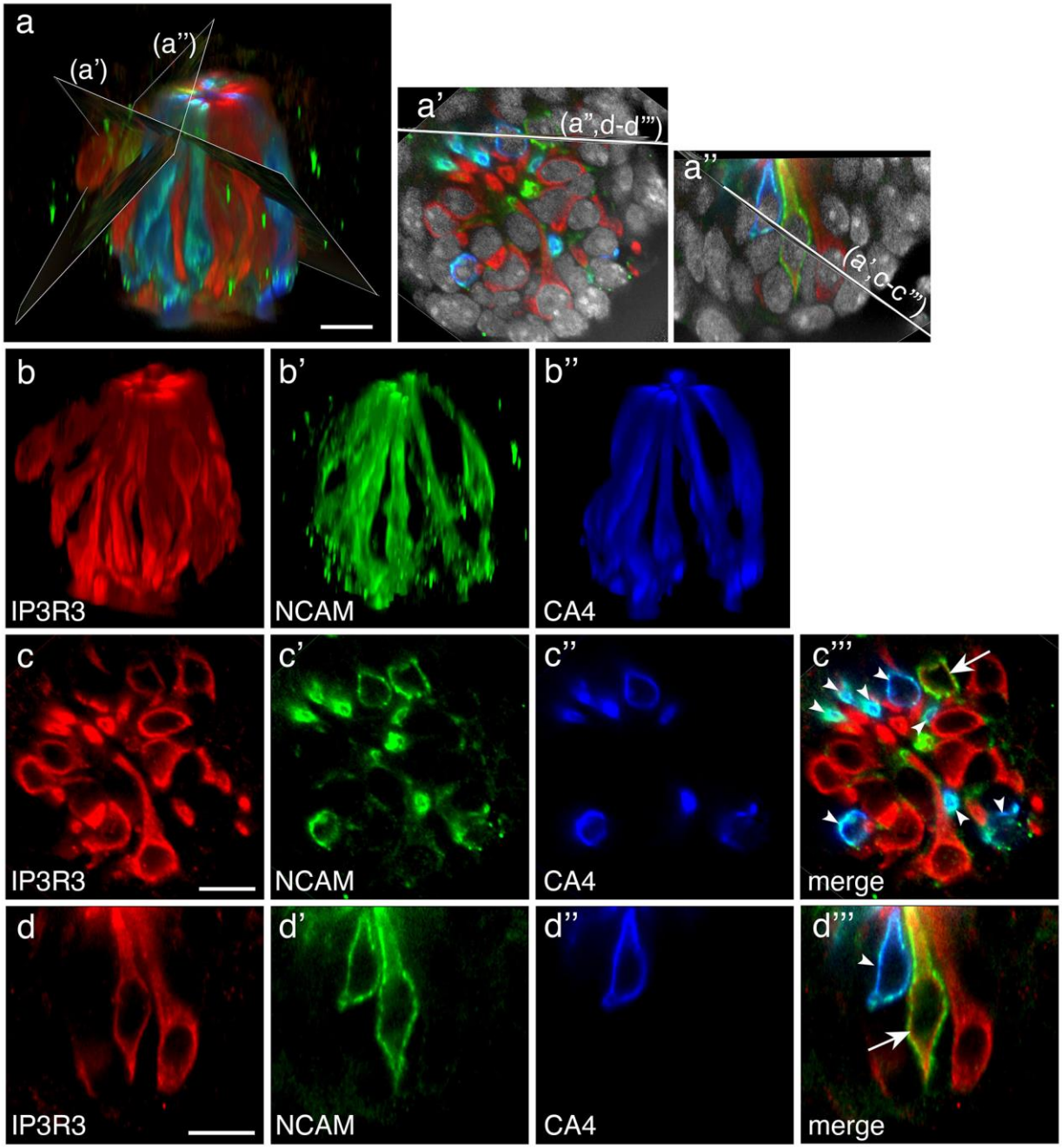

Fig. 3 Colocalization of IP3R3 and NCAM immunoreactivities in the SP. IP3R3 (red), NCAM (green) and CA4 (blue) were detected by whole mount immunohistochemistry. **a,b-b''** 3D-projection image of the taste bud and resliced sections [(a'),(a'')]. The basal side of taste buds to the bottom. **a'**,**a''** The resliced sections are perpendicular each other. In the slice images, the cutting plane of the other resliced section is shown by the white line marked with (a',c-c''') or (a'',d-d'''). The signals for nuclei detected by DAPI are shown in gray scale. **c-c'''** The resliced section (**a'**). **d-d'''** The resliced section (**a''**). The arrow indicates the cell expressing both IP3R3 and NCAM. The arrowhead indicates the cells co-expressing NCAM and CA4. Scaler bar, 10 μm.

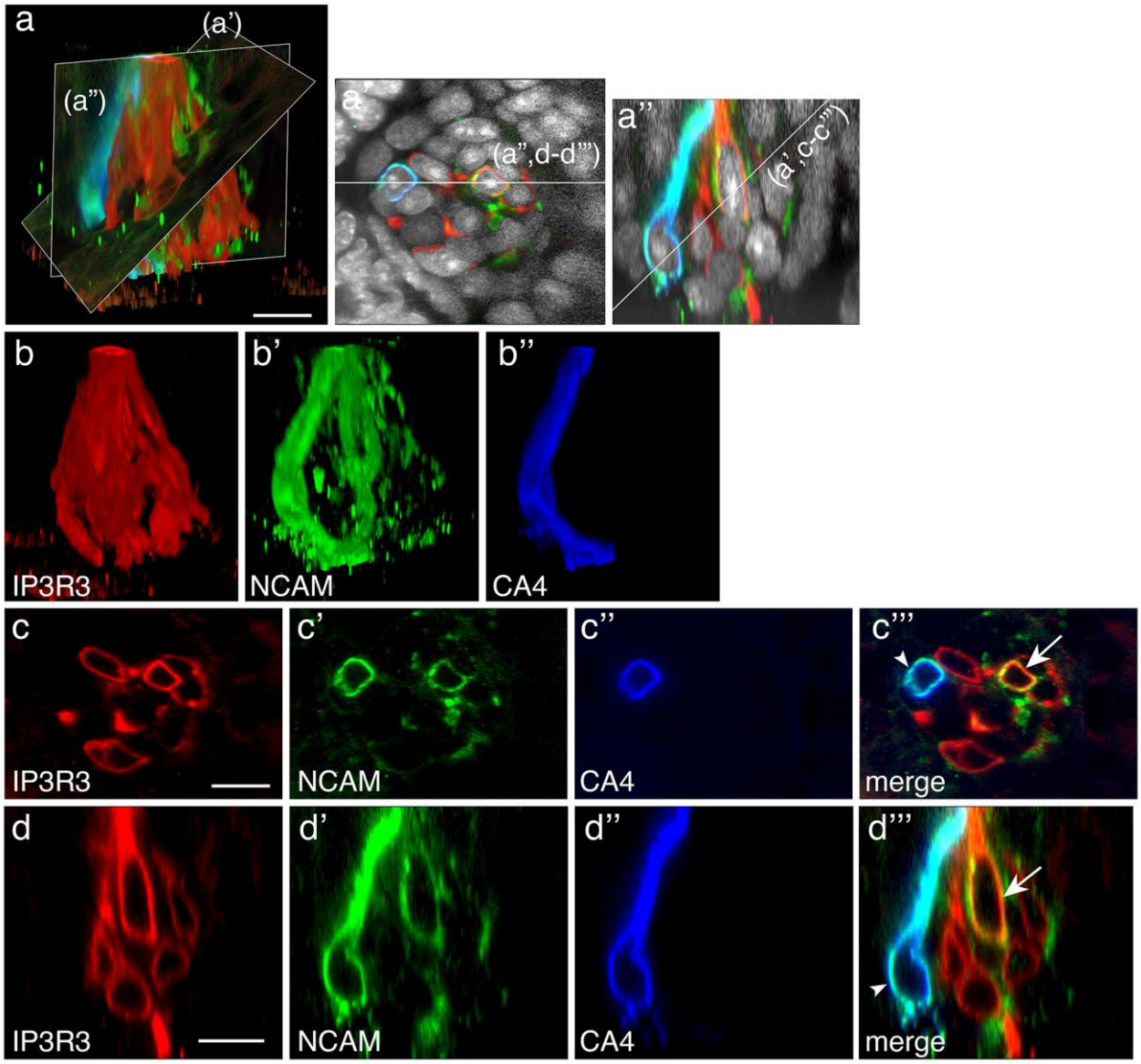

Fig. 4 Colocalization of IP3R3 and NCAM immunoreactivities in the FF. Legend is same as in Figure 3.

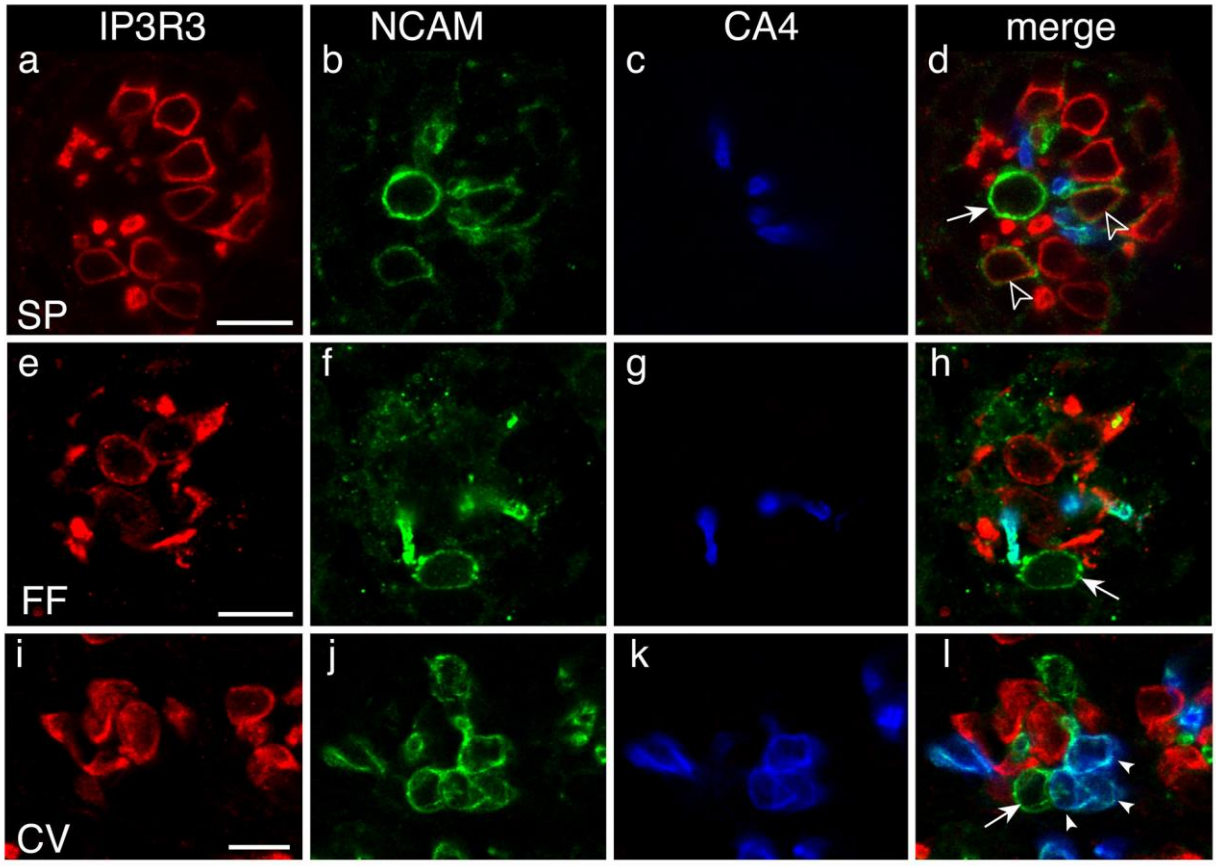

Fig 5 NCAM expression separated from IP3R3 and CA4 expression in the SP (**a**-**d**), FF (**e**-**h**) and CV (**i**-**l**). The arrow indicates the cells positive for NCAM (green) but negative for both IP3R3 (red) and CA4 (blue). The arrowhead indicates the cells co-expressing NCAM and CA4 in the CV. The outlined arrowhead indicates the cells co-expressing IP3R3 and NCAM in the SP. Scale bar, 10 μm.

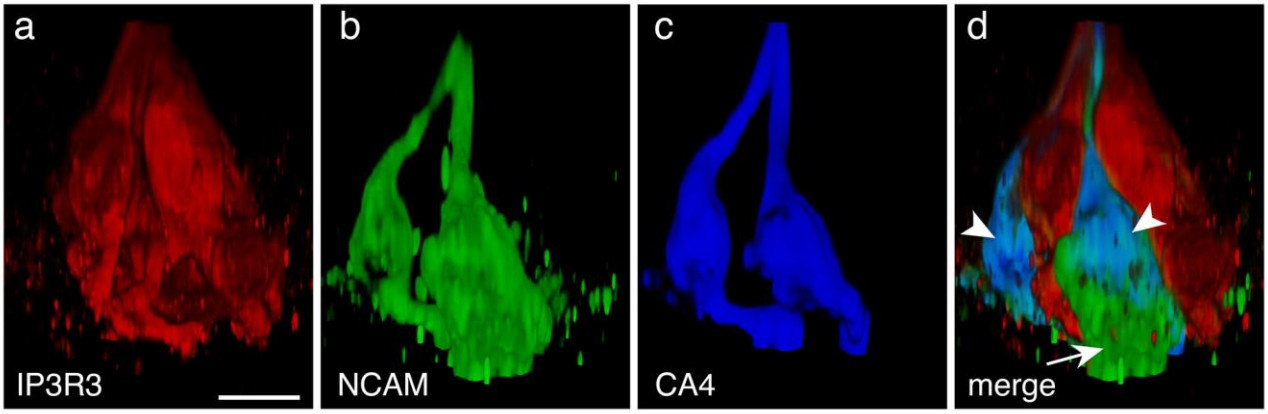

Fig. 6 3D-projecion image of the taste bud in the FF (**a**-**d**). The arrow indicates an example of the NCAM(+) cell (green) without CA4 (blue) or IP3R3 (red). The arrowhead indicates NCAM(+)CA4(+) cells. The basal side of taste bud to the bottom. Scale bar, 10 μm.

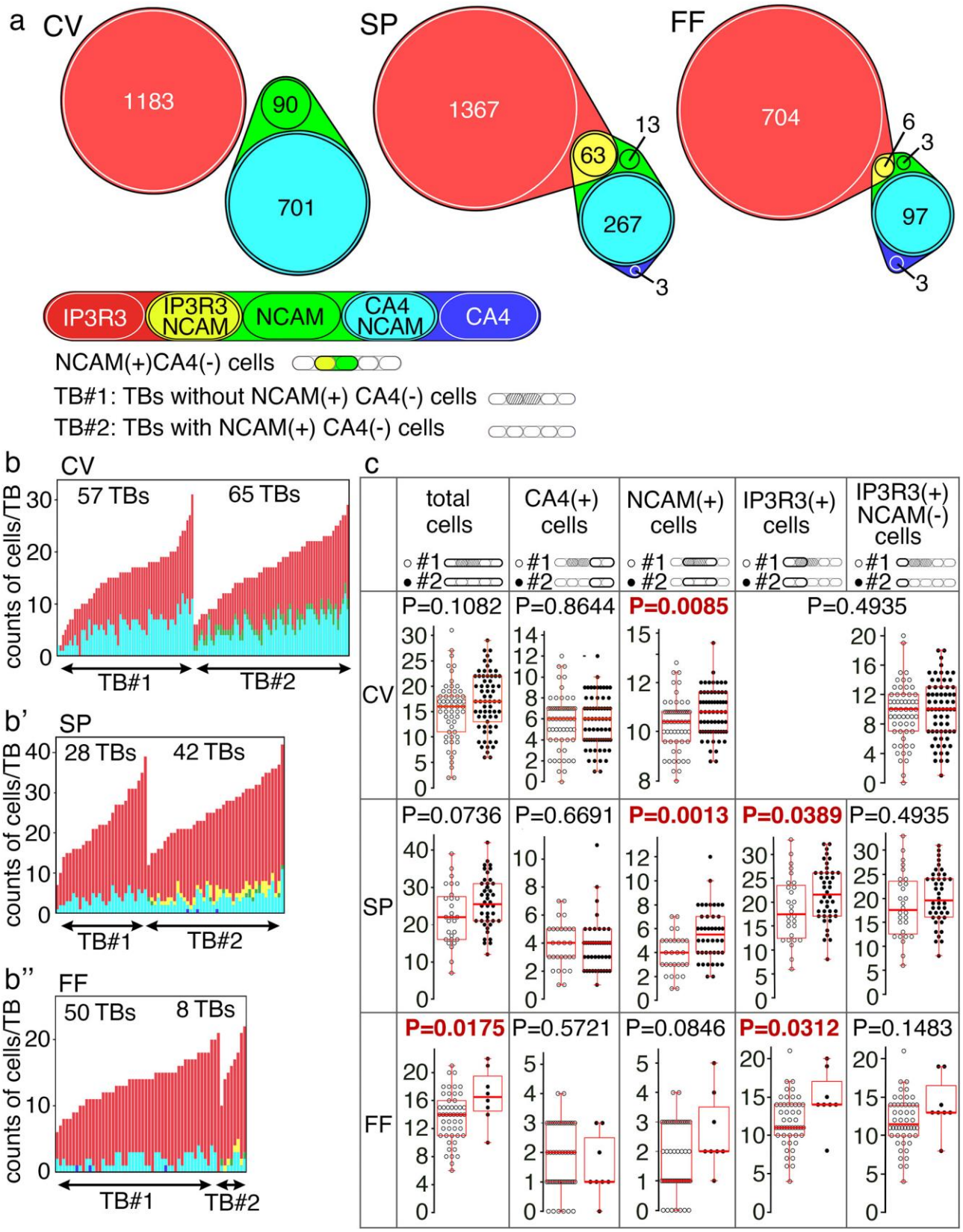
a
CV
1183
90
701
SP
1367
13
63
267
3
FF
704
6
3
97
3
IP3R3
IP3R3 NCAM
NCAM
CA4 NCAM
CA4
NCAM(+)CA4(-) cells
TB#1: TBs without NCAM(+) CA4(-) cells
TB#2: TBs with NCAM(+) CA4(-) cells
b
CV
57 TBs
65 TBs
counts of cells/TB
TB#1
TB#2
b'
SP
28 TBs
42 TBs
b''
FF
50 TBs
8 TBs
c
total cells
CA4(+) cells
NCAM(+) cells
IP3R3(+) cells
IP3R3(+) NCAM(-) cells
#1
#2
CV
SP
FF
P=0.1082
P=0.8644
P=0.0085
P=0.4935
P=0.0736
P=0.6691
P=0.0013
P=0.0389
P=0.4935
P=0.0175
P=0.5721
P=0.0846
P=0.0312
P=0.1483

Fig. 7 Quantitative summaries of IP3R3(+), CA4(+), and NCAM(+) cells in the CV, SP, and FF. **a** Area proportional Venn diagrams showing the colocalization relationships of the immunoreactivities for IP3R3, CA4, and NCAM in the taste buds of the CV, SP, and FF. The expression is color-coded in the same RGB color-system as in Figure 3-6: Red, IP3R3; Green, NCAM; Blue, CA4. Yellow (Red + Green) indicates positive for IP3R3 and NCAM but not for CA4. Cyan (Green + Blue) indicates positive for NCAM and CA4 but not for IP3R3 (see the graphical legend at the bottom of Figure 7**a**). IP3R3 and CA4 double-positive cells were not observed in any region. The numeral in the center of each circle indicates the numbers of cells identified in each category, and the area of the circle proportionally indicates the numbers of cells in respective populations in each region. In the CV, taste bud cells are divided into IP3R3(+) and NCAM(+) cell populations. CA4(+) cells are included in the NCAM(+) cell population. In the SP and FF, CA4(+) cells are also virtually included in NCAM(+) cells but with a few exceptions (blue), and the majority of NCAM(+)CA(-) cells are IP3R3(+) (yellow). **b-b''** Stacked column chats of the number of immunopositive cells detected in individual taste buds (TB) in the CV (**b**), SP (**b'**), and FF (**b''**). The color-coding is the same as in **a**. Taste buds were classified into two categories: TB#1, TBs without NCAM(+)CA4(-) cells (green and yellow), TB#2, TBs with NCAM(+)CA(-) cells. The legend symbol above the graphs, which consists of five small ellipses, is the same as in **a** but reduced. The hatched area in the legend symbol indicates the cells not existing in TB#1. In the stacked column charts, data were arranged in ascending order of total counts of cells per taste bud in TB#1 and TB#2, respectively. The numerals in the chart indicate the number of taste buds counted in TB#1 and TB#2, respectively. In TB#2, no obvious correlation was noted between the occurrence of NCAM(+)CA4(-) cells (green and yellow) and the total counts of cells per taste bud. **c** Comparison of the number of respective cells per taste bud between TB#1 and TB#2. The top row indicates the cells compared: Total cells, CA4(+) cells, NCAM(+) cells, IP3R3(+) cells, and IP3R3(+)NCAM(-) cells. White and black spots indicate TB#1 and TB#2, respectively, and the hatched area indicates the cell populations lacking in TB#1. In the schematic representation, the areas surrounded by bold lines indicate the respective cell populations. The vertical axis in the plots represents the cell counts per taste bud. The numeral on the top of each plot is P value of Mann-Whitney U test. P-values less than 0.05 are shown in red indicating statistically significant differences. General trends in differences between TB#1 and TB#2 seem to be shared between regions. The total number of cells tends to be higher in TB#2 than in TB#1, while the statistically significant difference was detected only in the FF. No differences were found in CA4(+) cells. The number of NCAM(+) cells was higher in TB#2 than in TB#1, while the statistically significant difference was not detected in the FF. The number of IP3R3(+) cells was higher in TB#2 than in TB#1, and no differences were noted in IP3R3(+)NCAM(-) cells between TB#1 and TB#2.